УДК 539.1

MEAN-FIELD APPROXIMATION FOR FINITE NUCLEI AND NUCLEAR MATTER

S. Shlomo

Cyclotron Institute, Texas A&M University, College Station, USA

We discuss a realistic case of fitting the values of the Skyrme parameters to an extensive set of experimental data on the ground-state properties of many nuclei ranging from normal to exotic ones. We include, in particular, the radii for valence neutron orbits and the breathing-mode energies for several nuclei. We further constrain the values of the Skyrme parameters by requiring positive values for the slope of the symmetry energy S, the enhancement factor, κ associated with the isovector giant dipole resonance, and the Landau parameter $G_0^{'}$. We also present results of Hartree-Fock based random phase approximation for the excitation strength function of the breathing mode and discuss the current status of the nuclear matter incompressibility coefficient.

1. Introduction

The nucleus is a fascinating and important laboratory for the study of properties of strongly interacting many body systems. Density functional theory, which is based on a theorem [1] for the existence of a universal energy density functional (EDF) that depends on the densities of the constituents and their derivatives, provides a powerful approach for theoretical calculations of properties of many body systems. However, the main challenge is to find the EDF. An important task of the nuclear physics community is to develop a modern EDF which accounts for the effects of few body and many body correlations and provides enhanced predictive power for properties of rare nuclei with unusual neutron-to-proton ratios that are difficult to produce experimentally and likely to exhibit interesting new phenomena associated with effects of isospin, clusterization, and the continuum.

Starting from the EDF associated with the Skyrme effective nucleon-nucleon interaction [2 - 6], we will present below a more realistic EDF with improved predictive power for properties of nuclei at and away from the valley of stability.

Since the pioneering work of Brink and Vautherin [4], continuous efforts have been made to readjust the parameters of the Skyrme-type effective nucleon-nucleon (NN) interaction to better reproduce experimental data [7]. Most of the parameters of the Skyrme interactions available in the literature were obtained by fitting the Hartree-Fock (HF) results to experimental data on bulk properties of a few stable closed-shell nuclei. Thus, it is desirable to have a unified interaction which includes the merits of several families of the Skyrme interactions, as already mentioned. One can further enhance the applicability of the Skyrme-type effective nucleon-nucleon interaction by imposing certain constraints, as subsequently discussed. Adopting the standard parameterization of Skyrme type interactions [4], we have recently determined within the Hartree - Fock (HF) approximation a new and more realistic Skyrme interaction (named KDE0) by fitting [8] a set of extensive data on binding energies, "bare" single particle energies, charge root mean square (rms) radii, and rms radii of valence nucleon density distribution of nuclei. We have included in the fit, for the first time, the data on the constraint energies of the isoscalar giant monopole resonances (ISGMR) of nuclei and imposed additional constraints, such as a non-negative value for the slope of the symmetry energy density at high nuclear matter (NM) density (at three times the saturation density of NM) and the Landau stability constraints on nuclear matter. We have implemented, for the first time, the simulated annealing method (SAM) together with an advanced least square method to search for the global minima. We have organized our presentation as follows. In Section 2 we briefly outline the form of the Skyrme NN effective interaction and the corresponding energy-density functional we have adopted in the present work. In this section, we also provide feasible strategies for the calculations Coulomb displacement energy (CDE) and the center of mass (CM) corrections to the total binding energy and charge rms radii. In Section 3 we describe the SAM algorithm. The set of the experimental data along with the theoretical errors and the constraints used in the fit to determine the values of the Skyrme parameters are given in Section 4. In Section 5 we present results for two different fits. In Section 6 we present the results of Hartree - Fock (HF) based random phase approximation (RPA) for the ISGMR and discuss the value of the NM incompressibility coefficient. In Section 7 we summarize our main results and discuss the scope for the further improvement of the EDF.

2. Skyrme energy density functional

We have adopted the following form for the Skyrme type effective NN interaction [4]:

$$V_{12} = t_0(1 + x_0\ P_{12}{}^{\sigma})\delta(\vec{r}_1 - \vec{r}_2) + \frac{1}{2}t_1(1 + x_1 P_{12}{}^{\sigma})[\vec{k}_{12}^2\delta(\vec{r}_1 - \vec{r}_2) + \delta(\vec{r}_1 - \vec{r}_2)\vec{k}_{12}^2] +$$
$$+t_2(1 + x_2 P_{12}{}^{\sigma})\vec{k}_{12}\delta(\vec{r}_1 - \vec{r}_2)\vec{k}_{12} + \frac{1}{6}t_3(1 + x_3 P_{12}{}^{\sigma})\rho^{\alpha}\left(\frac{\vec{r}_1 + \vec{r}_2}{2}\right)\delta(\vec{r}_1 - \vec{r}_2) + \quad (1)$$
$$+iW_0\vec{k}_{12}\delta(\vec{r}_1 - \vec{r}_2)(\vec{\sigma}_1 + \vec{\sigma}_2)\times\vec{k}_{12}.$$

where t_i, x_i, α, and W_0 are the parameters of the interaction and P_{12}^{σ} is the spin exchange operator, $\vec{\sigma}_i$ is the Pauli spin operator, $\vec{k}_{12} = -i\left(\vec{\nabla}_1 - \vec{\nabla}_2\right)/2$, and $\vec{k}_{12} = -i\left(\vec{\nabla}_1 - \vec{\nabla}_2\right)/2$. Here, the right and left arrows indicate that the momentum operators act on the right and on the left, respectively. The corresponding mean-field V_{HF} and the total energy E of the system are given by

$$V_{HF} = \frac{\delta H}{\delta\rho},\ \ E = \int H(r)d^3r, \quad (2)$$

respectively, where, the Skyrme energy-density functional *H(r)*, obtained using Eq. (1), is given by [4, 5],

$$H = K + H_0 + H_3 + H_{eff} + H_{fin} + H_{so} + H_{sg} + H_{Coul}, \quad (3)$$

where $K = \frac{\hbar^2}{2m}\tau$ is the kinetic-energy term, H_0 is the zero-range term, H_3 is the density dependent term, H_{eff} is an effective-mass term, H_{fin} is a finite-range term, H_{so} is a spin-orbit term, H_{sg} is a term that is due to tensor coupling with spin and gradient and H_{Coul} is the contribution to the energy-density that is due to the Coulomb interaction. For the Skyrme interaction of Eq. (1), we have

$$H_0 = \frac{1}{4}t_0\left[\left(2 + x_0\right)\rho^2 - \left(2x_0 + 1\right)\left(\rho_p^2 + \rho_n^2\right)\right], \quad (4)$$

$$H_3 = \frac{1}{24}t_3\rho^{\alpha}\left[\left(2 + x_3\right)\rho^2 - \left(2x_3 + 1\right)\left(\rho_p^2 + \rho_n^2\right)\right], \quad (5)$$

$$H_{eff} = \frac{1}{8}\left[t_1\left(2 + x_1\right) + t_2\left(2 + x_2\right)\right]\tau\rho + \quad (6)$$
$$+\frac{1}{8}\left[t_2\left(2x_2 + 1\right) - t_1\left(2x_1 + 1\right)\right]\left(\tau_p\rho_p + \tau_n\rho_n\right),$$

$$H_{fin} = \frac{1}{32}\left[3t_1\left(2 + x_1\right) - t_2\left(2 + x_2\right)\right](\nabla\rho)^2 - \quad (7)$$
$$-\frac{1}{32}\left[3t_1\left(2x_1 + 1\right) + t_2\left(2x_2 + 1\right)\right]\left[\left(\nabla\rho_p\right)^2 + \left(\nabla\rho_n\right)^2\right],$$

$$H_{so} = \frac{W_0}{2}\left[J\cdot\nabla\rho + x_w\left(J_p.\nabla\rho_p + J_n\cdot\nabla\rho_n\right)\right] \quad (8)$$

and

$$H_{sg} = -\frac{1}{16}\left(t_1x_1 + t_2x_2\right)J^2 + \frac{1}{16}\left(t_1 - t_2\right)\left[J_p^2 + J_n^2\right]. \quad (9)$$

Here, $\rho = \rho_p + \rho_n$, $\tau = \tau_n + \tau_n$ and $\boldsymbol{J} = \boldsymbol{J}_{\rm p} + \boldsymbol{J}_{\rm n}$ are the particle number density, kinetic-energy density and spin-density with p and n denoting the protons and neutrons, respectively. Note that the additional parameter x_w, introduced in Eq. (8), allows us to modify the isospin dependence of the spin-orbit term. The value of $\hbar^2/2m = 20.734$ MeV fm^2 was used in the calculations. We would like to emphasize that the contributions from the spin-density term as given by Eq. (9), which is ignored in many Skyrme HF calculations were included in these calculations. Although the contributions from Eq. (9) to the binding energy and charge rms radii are not very significant, they are very crucial for the calculation of the Landau parameter G_0'.

2.1. Coulomb energy

The contribution to the energy-density Eq. (3) from the Coulomb interaction can be written as a sum of a direct and an exchange terms:

$$H_{Coul}(r) = H_{Coul}^{dir}(r) + H_{Coul}^{ex}(r). \quad (10)$$

For the direct term it is common to adopt the expression

$$H_{Coul}^{dir}(r) = \frac{1}{2}e^2\rho_p(r)\int\frac{\rho_p(r')d^3r'}{\left|\vec{r} - \vec{r'}\right|} \quad (11)$$

and for the corresponding exchange term to use the Slater approximation:

$$H_{Coul}^{ex}(r) = -\frac{3}{4}e^2\rho_p(r)\left[\frac{3\rho_p(r)}{\pi}\right]^{1/3}. \quad (12)$$

It is very important to emphasize that the definitions of Eqs. (11) and (12) are not for the bona fide direct and exchange terms since each of them includes the contributions of the self-interaction term, which

appear in opposite signs and cancel out in Eq. (10), see Ref. [9].

We recall that within the mean-field approximation, adjusted to reproduce the experimental values of the charge rms radii, the calculated CDE of analog states (obtained using Eq. (10)) are smaller than the corresponding experimental values by about 7 %. It was first shown in Ref. [10] that this discrepancy, also known as the Nolen - Schiffer anomaly [11], can be explained when the contributions that are due to long-range correlations (LRCs) and those due to the charge symmetry breaking (CSB) in the NN interaction are taken into account. We note that by neglecting the term of Eq. (12), one neglects the bona fide Coulomb exchange term together with the spurious contribution of the self-interaction term. These results in a contribution to CDE that is similar in magnitude to the contributions obtained from the LRC + CSB terms.

2.2. Center-of-mass corrections to the binding energy and charge rms radii

The HF approach applied to finite nuclei violates the translational invariance, introducing a spurious CM motion. Thus, one must extract the contributions of the CM motion to the binding energy B, rms radii and other observables. To account for the CM correction to the total binding energy, one must subtract from it the so-called CM energy given as,

$$E_{CM} = \frac{1}{2mA}\left\langle \hat{P}^2 \right\rangle \qquad (13)$$

where, $P = -i\hbar\sum\nabla_i$ is the total linear momentum operator. Traditionally, one simplifies the computation of Eq. (13) by taking into account only the one-body parts of it, which can be easily achieved by replacing $\frac{1}{m} \to \frac{1}{m}\left[1-\frac{1}{A}\right]$ in the kinetic-energy term. In this case, the effects of neglecting the two-body part of Eq. (13) are compensated by renormalization of the force parameters. This may induce in the forces an incorrect trend with respect to A that becomes visible in the nuclear matter properties. Thus an appropriate and still simple scheme to evaluate Eq. (13) is highly desirable.

A simple but more consistent scheme to evaluate the energies of the CM was employed by adopting the harmonic oscillator (HO) approximation $E_{CM}^{HO} = \frac{3}{4}\hbar\omega$, and determining the oscillator energy $\hbar\omega$ using the mean-square mass radii $\left\langle r^2 \right\rangle$ calculated in the HF approach as

$$\hbar\omega = \frac{\hbar^2}{mA\left\langle r^2 \right\rangle}\sum_i\left[N_i + \frac{3}{2}\right], \qquad (14)$$

where the sum runs over all the occupied single-particle states for the protons and neutrons and N_i is the oscillator quantum number. We emphasize that this scheme is quite reliable even for the nuclei away from the β-stability line, where the values of the rms radii deviate from the $A^{1/3}$ law.

The corresponding mean-square charge radius to be fitted to the experimental data is obtained as

$$\left\langle r_{ch}^2 \right\rangle = \left\langle r_p^2 \right\rangle_{HF} - \frac{3}{2\nu A} + \left\langle r^2 \right\rangle_p + \frac{N}{Z}\left\langle r^2 \right\rangle_n +$$

$$+\frac{1}{Z}\left(\frac{\hbar}{mc}\right)\sum_{nlj\tau}(2j+1)\mu_\tau\left\langle \vec{\sigma}.\vec{l} \right\rangle_{lj}, \qquad (15)$$

where $\left\langle r^2 \right\rangle_p$ and $\left\langle r^2 \right\rangle_n$ are the mean-squared radii of the proton and neutron charge distributions, respectively. The second term in Eq. (15) is due to the CM motion, with $\nu = m\omega/\hbar$ being the HO size parameter. The last term in Eq. (15) is due to the electromagnetic spin-orbit effect. We use the experimental value $\left\langle r^2 \right\rangle_n = -0.12$ fm^2 and the (recent) experimental value $\left\langle r^2 \right\rangle_p = 0.801$ fm^2.

2.3. Determination of the critical density

The Landau stability conditions of the NM are given as [12]

$$A_l > -(2l+1), \qquad (16)$$

where A_l stands for the Landau parameters F_l, F_l', G_l and G_l' for a given multipolarity l. Skyrme interactions contain only monopolar and dipolar contributions to the particle-hole interaction so that all Landau parameters are zero for $l > 1$. Thus, there are 12 different Landau parameters, i.e., F_l, F_l', G_l and G_l' (l = 0, 1) for the symmetric nuclear matter and $F_l^{(n)}, G_l^{(n)}$ (l = 0, 1) for the pure neutron matter. The critical density ρ_{cr} is defined as the maximum density beyond which at least one of the Landau parameters does not satisfy Eq. (16). Following Ref. [13], one can obtain the values of the Landau parameters at any density for a given set of the Skyrme parameters. We included the quantity ρ_{cr} in the fit.

2.4. Breathing-mode energy

We have considered the fully self-consistent values for the breathing-mode constraint energy, defined as

$$E_0 = \sqrt{\frac{m_1}{m_{-1}}}, \qquad (17)$$

where m_k are the energy moments

$$m_k = \int_0^\infty \omega S(\omega) d\omega \qquad (18)$$

of the strength function

$$S(\omega) = \sum_n \left|\left\langle n\left|F\right|0\right\rangle\right|^2 \delta(\omega - \omega_n) \qquad (19)$$

for the monopole operator $F(r) = \sum_{i=1}^{A} f(r_i)$, with $f(r) = r^2$. The moments m_{-1} and m_1 appearing in Eq. (17) can be obtained using the constrained HF (CHF) and the double commutator sum rule, respectively [8], as

$$m_1 = 2\frac{\hbar^2}{m}\left\langle r^2\right\rangle \quad \text{and} \quad m_{-1} = \frac{1}{2}\frac{d}{d\lambda}\left\langle r_\lambda^2\right\rangle_{\lambda=0}, \qquad (20)$$

where

$$\left\langle r^2\right\rangle = \int r^2 \rho(r) d\vec{r}\,. \qquad (21)$$

In Eq. (20), $\left\langle r_\lambda^2\right\rangle = \left\langle \Phi_\lambda \left| r^2 \right| \Phi_\lambda \right\rangle$; where Φ_λ being the HF solution to the CHF Hamiltonian $H - \lambda f$. The experimental data for the constraint energy E_0 was included in the fit.

3. Simulated annealing based algorithm for the minimization of χ^2

We have implemented the simulated-annealing method (SAM) to search for the global minimum of the χ^2 function as given by

$$\chi^2 = \frac{1}{N_d - N_p}\sum_{i=1}^{N_d}\left(\frac{M_i^{\exp} - M_i^{th}}{\sigma_i}\right)^2, \qquad (22)$$

where N_d and N_p are the number of experimental data points and the number of fitted parameters, respectively, σ_i is the theoretical error, and $M_i^{\exp}$ and M_i^{th} are the experimental and the corresponding HF theoretical values, respectively, for a given observable.

From the literature [7] one finds that the Skyrme parameters vary over a wide range. Therefore, to make the search process more efficient, we take advantage of the fact that the Skyrme parameters can be expressed in terms of the various quantities which are related to the nuclear matter, since these nuclear matter quantities are known empirically within 10 - 20 %. For convenience, we have defined a vector v with the components as

$$v \equiv \left(B/A, K_{nm}, \rho_{nm}, m^*/m, E_s, J, L, \kappa, G_0^{'}, W_0\right). \qquad (23)$$

Here $B/A, K_{nm}, \rho_{nm}, m^*/m, E_s, J, L, \kappa, G_0^{'}$, and W_0 are the binding energy per nucleon, NM incompressibility coefficient, nuclear matter density, effective mass, surface energy, symmetry energy coefficient, the quantity which is related to the slope of the symmetry energy coefficient ($L = 3\rho dJ/d\rho$), the enhancement factor in the energy weighted sum rule (EWSR) of the isovector giant dipole resonance (IVGDR), Landau parameter, and the Skyrme spin-orbit parameter, respectively.

Once the vector v is known one can calculate the values of all the Skyrme parameters. We have also defined the vectors v_0, v_1 and d. The vector v_0 and v_1 contain the lower and the upper limits of each of the components of the vector v. The vector d represents the maximum displacement allowed in a single step for the components of the vector v. For a given set of experimental data, we have implemented the SAM algorithm using the following basic steps:

(i) Starting with a guess for the vector v we calculate χ^2 (say, χ^2_{old}) using Eq. (22).

(ii) We first use a uniform random number to select a component v_r of the vector v, and then the randomly selected component v_r is then assigned a new value

$$v_r \to v_r + \eta d_r \qquad (24)$$

where η is a uniform random number that lies within the range of -1 to +1. The second step is repeated until the new value of v_r is found within its allowed limits defined by v_0 and v_1. We use this modified v to generate a new set of Skyrme parameters.

(iii) We calculate the quantity

$$P\left(\chi^2\right) = e^{\left(\chi^2_{old} - \chi^2_{new}\right)/T}, \qquad (25)$$

where χ^2_{new} is obtained by using the newly generated set of the Skyrme parameters and T is an effective temperature. The new set of Skyrme parameters is accepted only if

$$P\left(\chi^2\right) > \beta, \tag{26}$$

where β is a uniform random number that lies between 0 and 1. If the new Skyrme parameters are accepted, it is called a "successful reconfiguration". To search for the global minimum of χ^2 we begin with some reasonable value of an effective temperature $T = T_i$. For a given T_i, we repeat steps (ii) and (iii) for, say, $100N_p$ reconfigurations, or for $10\ N_p$ successful reconfigurations, which ever comes first. Then, we reduce the temperature by following the Cauchy annealing schedule given by

$$T(k) = T_i / ck \tag{27}$$

where c is a constant, which is taken to be a unity, and k = 1; 2; 3; … is the time index. We keep on reducing the value of T by using Eq. (27) in the subsequent steps until the effort to reduce the value of χ^2 further becomes sufficiently discouraging.

4. Experimental data and some constraints

In Table 1 we summarize the choice of the experimental data. It must be noted that, in addition to the typically used data on the binding energy, charge rms radii and spin-orbit splitting, we have also included in our fit the experimental data for the rms radii of valence neutron orbits and the breathing-mode constraint energies of several nuclei. For the binding energy we have used in the fit the error of 1.0 MeV except for the ^{100}Sn nuclei, in which we have used 2.0 MeV since the binding energy for the ^{100}Sn nucleus is determined from systematics. For the charge rms radii we have adopted the theoretical error of 0.02 fm except for the case of ^{56}Ni nucleus. The charge rms radius for the ^{56}Ni nucleus is obtained from systematic and we use the theoretical error of 0.04 fm. We considered in the fit the experimental data for the spin-orbit splittings for the 2p neutrons and protons in the ^{56}Ni nucleus and the rms radii for the $1d_{5/2}$ and $1f_{7/2}$ neutron orbits in ^{17}O and ^{41}Ca nuclei, respectively. The theoretical error taken for the spin-orbit splitting data is 0.2 MeV, and for the rms radii for the valence neutron orbits the experimental error of 0.06 fm was adopted. To be consistent with the way these valence neutron radii are determined, the CM correction to these data was not included. The experimental data for the breathing-mode constraint energies E0 for the ^{90}Zr, ^{116}Sn, ^{144}Sm and ^{208}Pb nuclei were included in the fit with the theoretical error taken to be 0.5 MeV for the ^{90}Zr nucleus and 0.3 MeV for the other nuclei. We have also included the critical density ρ_{cr} in the fit, assuming a value of $2.5\,\rho_0$ with an error of $0.5\,\rho_0$. Further the values of the Skyrme parameters were constrained by requiring (i) a positive slope for the symmetry energy density for $\rho \le 3\rho_0$, (ii) $\kappa = 0.1 - 0.5$ and (iii) $G_0' \ge 0$ at $\rho = \rho_0$ (see Ref. [8] for details).

Table 1. **Selected experimental data for the binding energy B, charge rms radius r_{ch}, rms radii of valence neutron orbits r_v, spin-orbit splitting S-O, breathing-mode constraint energy E_0, and critical density ρ_{cr} used in the fit to determine the parameters of the Skyrme interaction**

Properties	Nuclei
B	^{16,24}O, ^{34}Si, ^{40,48}Ca, ^{48,56,68,78}Ni, ^{88}Sr, ^{90}Zr, ^{100,132}Sn, ^{208}Pb
r_{ch}	^{16}O, ^{40,48}Ca, ^{56}Ni, ^{88}Sr, ^{90}Zr, ^{208}Pb
$r_v(\nu 1f_{5/2})$	^{17}O
$r_v(\nu 1f_{7/2})$	^{41}Ca
S-O	2p orbits in ^{56}Ni
E_0	^{90}Zr, ^{116,132}Sn, ^{144}Sm, ^{208}Pb
ρ_{cr}	Nuclear matter

5. Results and discussions

Two different fits were carried out [8] and are named as (i) KDE0, in which only the Coulomb direct term in the form of Eq. (11) is included; and KDE, in which the direct as well as the Coulomb exchange terms are included, Eqs. (10) - (12). It was found that T_i = 1.25, along with the Cauchy annealing schedule as given by expression (47), yields reasonable values for the best-fit parameters. To validate this approach the following checks were made. Starting with the final values of the Skyrme parameters obtained using the SAM, a minimization of the value of χ^2 using the Levenberg-Marquardt (LM) method [14] was carried out. We plot in Fig. 1 the average value $\left\langle \chi^2 \right\rangle_T$ as a function of the inverse of the control parameter T for the KDE0 case. The curves labeled v and v1 represent the results obtained from two different choices of the starting values for the Skyrme parameters. The value of $\left\langle \chi^2 \right\rangle_T$ is obtained by averaging over all the successful reconfigurations for a given T. We see from Fig. 1 that the value of $\left\langle \chi^2 \right\rangle_T$ shows a remarkable decrease at initial stages and then oscillates before saturating to a minimum value for $T \le 0.05$. The value of $\left\langle \chi^2 \right\rangle$ at lower T is more or less independent of the starting values for the Skyrme parameters.

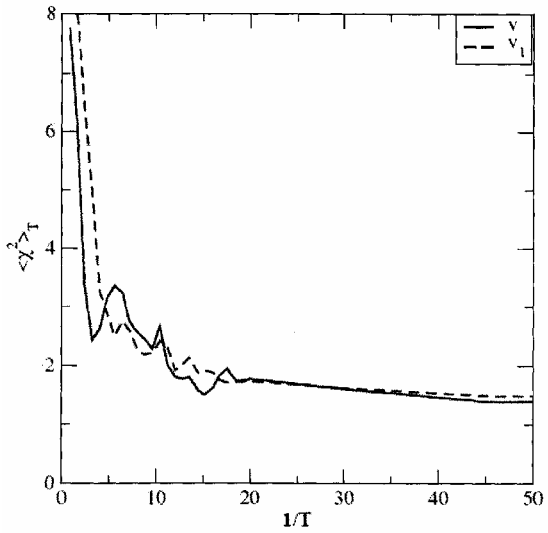

Fig. 1. Variation of the average value of chi-square, $\langle \chi^2 \rangle T$, as a function of the inverse of the control parameter T for the KDE0 interaction for the two different choices of the starting parameters.

In Table 2 we give the values for the resulting Skyrme parameters together with the various quantities characterizing the nuclear matter obtained at the minimum value of the $\langle \chi^2 \rangle$ for the KDE0 and KDE Skyrme interactions. We also give in parenthesis the values of the standard deviations for the Skyrme parameters. The values of the standard deviations on the parameters for the KDE0 and KDE interactions were determined by using the LM method.

In Table 3 we present the results for the deviations $\Delta B = B^{\exp} - B^{th}$ and $\Delta r_{ch} = r_{ch}^{\exp} - r_{ch}^{\exp}$ for the values of the binding energy and charge rms radii, respectively, obtained from the newly generated KDE0 and KDE interactions. One can easily verify from Table 3 that in the case of the KDE) interaction the magnitude of the deviations for the binding energy for most nuclei are much less than 0.5 %. The KDE interaction yields larger error in the values of the binding energy (~ 0.6 - 1.0 %) for the ^{16}O, ^{48}Ni and ^{100}Sn nuclei. We also see from Table 3 that, except for the ^{16}O and ^{48}Ca nuclei, the deviations in the values of the charge rms radii for the KDE0 interaction are less than 0.5 %.

Table 2. **The values of the Skyrme parameters and the corresponding physical quantities of nuclear matter parameters for KDE0 and KDE interactions obtained by minimizing the $\langle \chi^2 \rangle$. The values in Parenthesis are the standard deviation for the corresponding Skyrme parameters**

Parameter	KDE0	KDE
t_0(MeV.fm^3)	-2526.5110 (140.6256)	-2532.8842 (115.3165)
t_1 (MeV.fm^5)	430.9418 (16.6729)	403.7285 (27.6336)
t_2 (MeV.fm^5)	-398.3775 (27.3099)	-394.5578 (14.2610)
t_3 (MeV_fm$^{3(1+\alpha)}$)	14235.5193 (680.7344)	14575.0234 (641.9932)
x_0	0.7583 (0.0655)	0.7707 (0.0579)
x_1	-0.3087 (0.0165)	-0.5229 (0.0298)
x_2	-0.9495 (0.0179)	-0.8956 (0.0270)
x_3	1.1445 (0.0862)	1.1716 (0.0767)
W_0 (MeV.fm^5)	128.9649 (3.3258)	128.0572 (4.3943)
A	0.1676 (0.0163)	0.1690 (0.0144)
B/A (MeV)	16.11	15.99
K_{nm} (MeV)	228.82	223.89
ρ_{nm}	0.161	0.164
m*/m	0.72	0.76
E_s (MeV)	17.91	17.98
J (MeV)	33.00	31.97
L (MeV)	45.22	41.43
K_{nm}	0.30	0.16
$G_0^{'}$	0.05	0.03
χ^2_{min}	1.3	2.2

Table 4 shows that the results for the values of ρ_{cr}, the values for the rms radii of valence neutron orbits, the spin-orbit splittings and the breathing mode constraint energies, considered in the fits, are quite reasonable for the two interactions considered here. It can be also seen from Table 4 that the fit to the breathing-mode constraint energies are overall in reasonable agreement with the corresponding experimental data.

Table 3. **Results for the total binding energy B (in MeV) and charge rms radii r_{ch} (in fm) for several nuclei. Also given the corresponding derivations from the experimental values; $\Delta B = B^{\exp} - B^{th}$ and $\Delta r_{ch} = r_{ch}^{\exp} - r_{ch}^{th}$**

		$\Delta B = B^{\exp} - B^{th}$			$\Delta r_{ch} = r_{ch}^{\exp} - r_{ch}^{th}$	
Nuclei	$B^{\exp}$	KDE0	KDE	$r^{\exp}$	KDE0	KDE
^{16}O	127.620	0.394	1.011	2.730	-0.041	-0.039
^{24}O	168.384	-0.581	0.370			
^{34}Si	283.427	-0.656	0.060			
^{40}Ca	342.050	0.005	0.252	3.49	0.000	0.011
^{48}Ca	415.990	0.188	1.165	3.480	-0.021	-0.008
^{48}Ni	347.136	-1.437	-3.67			
^{56}Ni	483.991	1.091	1.106	3.750	-0.018	0.000
^{68}Ni	590.408	0.169	0.539			
^{78}Ni	641.940	-0.252	0.763			
^{88}Sr	768.468	0.826	1.132	4.219	-0.002	0.019
^{90}Zr	783.892	-0.127	-0.200	4.258	-0.008	0.013
^{100}Sn	824.800	-3.664	-4.928			
^{132}Sn	1102.850	-0.422	-0.314			
^{208}Pb	1636.430	0.945	-0.338	5.500	0.011	0.041

Table 4. **Critical density rms radii of the valence neutron orbits, spin-orbit splitting (S-O), and the breathing mode constraint energies. In the columns 3-4 we give the results obtained from KDE0 and KDE interaction respectively**

	Experimental	KDE0	KDE
ρ_{cr}/ρ_0	2.5	2.5	2.1
$r_v(\nu 1d_{5/2})(fm)$	3.36	3.42	3.41
$r_v(\nu 1d_{7/2})(fm)$	3.99	4.05	4.03
$\varepsilon_n(2p_{1/2}) - \varepsilon_n(2p_{3/2})(MeV)$	1.88	1.84	1.81
$\varepsilon_p(2p_{1/2}) - \varepsilon_p(2p_{3/2})(MeV)$	1.83	1.64	1.63
E_0 ^{90}Zr	17.81	17.98	17.91
^{116}Sn	15.90	16.42	16.36
^{144}Sm	15.25	15.53	15.47
^{208}Pb	14.18	13.64	13.60

6. Fully self-consistent HF based RPA

As an application of the newly determined KDE0 Skyrme interaction we now present results for the response function for the ISGMR for several nuclei.

The basic theory for microscopic description of different modes of giant resonances is the HF based RPA [15, 16]. Although this approach is conceptually well understood, actual calculations make compromises for reasons of simplicity or numerical expense. Unfortunately, apart from some fully self-consistent calculations, most of earlier HF-RPA calculations are contaminated by self consistent violations (SCV). It was pointed out [17] that the SCV associated with the omission of the p-h spin-orbit and Coulomb interactions may cause an error in E0 of the ISGMR which becomes larger than 1 MeV, i.e. as large as 5 times the experimental error. It is important to point out that neglecting the p-h spin-orbit interaction in the RPA calculation leads to an increase of E0 of ^{208}Pb by about 0.8 MeV, and therefore to an increase of ~ 30 MeV in the value extracted for $K_{\rm nm}$. We thus explained the discrepancy [18] in the value deduced for $K_{\rm nm}$ using Skyrme type or Gogny type effective interactions.

In Fig. 2 we present the results of fully self-consistent HF-based RPA calculations for the ISGMR (breathing mode) for several nuclei using the newly determined KDE0 interaction. We also show for comparison the results obtained using the SGII [19] interaction. We add that recently we have constructed the parameter set SK255 [20] of the Skyrme interaction, having $K_{\rm nm}$ = 255 MeV, which yields for the ISGMR centroid energies E0 values which are quite close to the relativistic mean field based RPA (RRPA) results obtained using the NL3 interaction which is associated with $K_{\rm nm}$ = 272 MeV. Moreover, for the SK255 parameter set, one finds a good agreement with experimental data for E0 for all the nuclei considered, provided, the corresponding excitation energy ranges used in determining E0 are the same as those used in obtaining the experimental data. We have thus resolved the discrepancy in the extracted value of

K_{nm} within relativistic and non-relativistic models [20] and conclude that the difference in the extracted values of K_{nm} is mainly due to the differences in the values of the symmetry energy coefficient J and its slope L associated with these models (see also Ref. [21]).

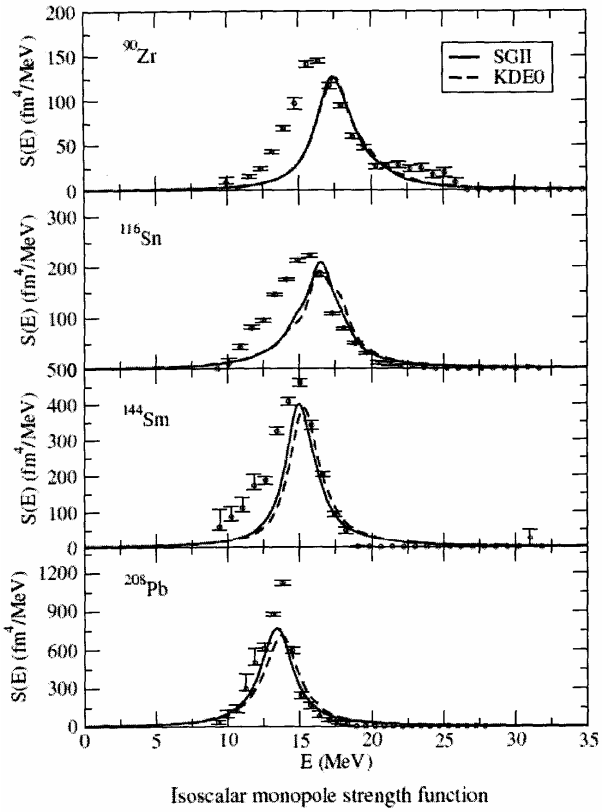

Fig. 2. Fully self-consistent HF-RPA results for the ISMGR strength functions of ^{90}Zr, ^{116}Sn, ^{144}Sm, and ^{208}Pb obtained using the interactions SGII and KDE0 and compared with the experimental data (cireles with error bars) [28].

7. Conclusions

We have employed the SAM to fit the values of the parameters of the Skyrme interaction. We have fitted an extensive set of experimental data together with a few additional constraints. The experimental data set consists of the binding energies for 14 nuclei ranging from the normal to exotic (proton- or neutron-rich) ones, charge rms radii for 7 nuclei, spin-orbit splittings for the 2p proton and neutron orbits of the ^{56}Ni nucleus, and rms radii for $1d_{5/2}$ and $1f_{7/2}$ valence neutron orbits in the ^{17}O and ^{41}Ca nuclei, respectively. We have also included in the fit the experimental data on the constraint energies of the ISGMR and the critical density ρ_{cr} determined from the stability conditions for the Landau parameters. The additional constraints imposed on the Skyrme parameters were: (i) the quantity $P = 3\rho(dS/d\rho)$, which is directly related to the slope of the symmetry energy S, must be positive for densities up to $3\rho_0$, a condition imposed by the neutron star models [22]; (ii) the enhancement factor κ, associated with the EWSR for the isovector giant dipole resonance, should lie in the range of 0.1 - 0.5; and (iii) the Landau parameter G_0', crucial for the spin properties of finite nuclei and nuclear matter, should be positive at $\rho = \rho_0$.

Using these experimental data along with the additional constraints, we have carried out two different fits named as KDE0 and KDE. The corrections to the binding energy and charge rms radii due to the CM motion were performed using simple but consistent schemes. The selection of the experimental data in conjugation with some constraints ensures that these interactions can be used to study the bulk ground-state properties of nuclei ranging from the stable to the ones near the proton and neutron drip lines, as well as the properties of neutron stars.

We have also presented results of fully self-consistent HF based RPA calculations of the ISGMR strength function using the newly determined KDE0 Skyrme effective interactions and compared them with those obtained using the SGII interactions. In conclusion:

(i) We have presented a new Skyrme effective interaction (KDE0) which should be applicable in the study of ground state properties of nuclei, ranging from stable to the ones near the drip lines, as well as properties of neutron stars.

(ii) We have also find that (see the review in Ref. [23]) that $K_{nm} = 240 \pm 20$ MeV. The uncertainty of 20 MeV is mainly due to the uncertainty in the value of J.

The effects on the binding energy and rms radii due to correlations beyond mean-field [24, 26, 27] can be included in the fit. These effects are, in particular, important for the light nuclei. One may also include in the spin-orbit splitting, the contributions due to the electromagnetic spin-orbit interaction [25] and properly account for the isospin dependence of the spin-orbit interaction. Last but not least, one may also include the experimental data on the giant dipole and quadrupole resonances while fitting the Skyrme parameters in addition to the breathing-mode energy, as was done in the present work.

Acknowledgments

This work was supported in part by the US National Science Foundation under Grant No. PHYS-0355200 and by the US Department of Energy under Grant No. DOE-FG03-93ER40773. The author thanks B. K. Agrawal, V. K. Au and D. C. Fuls for discussions and collaborations.

REFERENCES

1. *Kohn W.* // Rev. Mod. Phys. - 1999. - Vol. 71. - P. 1253.
2. *Skyrme T. H. R.* // Phil. Mag. - 1956. - Vol. 1. - P. 1043.
3. *Skyrme T. H. R.* // Nucl. Phys. - 1959. - Vol. 9. - P. 615.
4. *Vautherin D., Brink D. M.* // Phys. Rev. - 1972. - Vol. C5. - P. 626.
5. *Chabanat E., Bonche P., Haensel P. et al.* // Nucl. Phys. - 1997. - Vol. A627. - P. 710.
6. *Chabanat E., Bonche P., Haensel P. et al.* // Nucl. Phys. - 1998. - Vol. A635. - P. 231.
7. *Bender M., Heenen P. H., Reinhard P.-G.* // Rev. Mod. Phys. - 2003. - Vol. 75. - P. 121.
8. *Agrawal B. K., Shlomo S., V. K. Au* // Phys. Rev. - 2005. - Vol. C72. - P. 014310.
9. *Shlomo S.* // Rep. Prog. Phys. - 1978. - Vol. 41. - P. 957.
10. *Shlomo S., Love W. G.* // Physica Scripta. - 1982. - Vol. 26. - P. 280.
11. *Nolen J. A., Schiffer J. P.* // Annu. Rev. Nucl. Sci. - 1969. - Vol. 19. - P. 471.
12. *Migdal B.* Theory of Finite Fermi Systems, and Application to Atomic Nuclei. - New York: Interscience Pub., 1967.
13. *Margueron J., Navarro J., Giai N. V.* // Phys. Rev. - 2002. - Vol. C66. - P. 014303.
14. *Press W. H., Teukolsky S. A., Vetterling W. T., Flannery B. P.* Numerical Recipes in Fortran. - Cambridge: Cambridge University Press, 1992.
15. *Bohr A., Mottelson B. R.* Nuclear Structure. Vol. I. - New York: Benjamin, 1969.
16. *Shlomo S., Bertsch G. F.* // Nucl. Phys. - 1975. - Vol. A243. - P. 507.
17. *Agrawal B. K., Shlomo S., V. K. Au* // Phys. Rev. 2004. - Vol. C70. - P. 057302.
18. *Giai N. V., Bortignon P.F., Colo G. et al.* // Nucl. Phys. - 2001. - Vol. A687. - P. 44c.
19. *Giai N. V., Sagawa H.* // Phys. Lett. - 1981. - Vol. B106. - P. 379.
20. *Agrawal B. K., Shlomo S., Au V. K.* // Phys. Rev. - 2003. - Vol. C68. - P. 031304R.
21. *Piekarewicz J.* // Phys. Rev. - 2002. - Vol. C66. - P. 034305.
22. *Stone J. R., Miller J. C., Koncewicz R. et al.* // Phys. Rev. - 2003. - Vol. C68. - P. 034324.
23. *Shlomo S., Kolomietz V. M, Colo G.* // Eur. Phys. J. - 2006. - Vol. A30. - P. 23.
24. *Shlomo S.* // Phys. Lett. - 1988. - Vol. B209. - P. 23.
25. *Trache L., Kolomiets A., Shlomo S. et al.* // Phys. Rev. - 1996. - Vol. C54. - P. 2361.
26. *Esbensen H., Bertsch G. F.* // Phys. Rev. - 1983. - Vol. C28. - P. 355.
27. *Bender M., Bertsch G. F., Heenen P.-H.* // Phys. Rev. - 2004. - Vol. C69. - P. 034340.
28. *Youngbood D. H., Lui Y. W., Clark H. L. et al.* // Phys. Rev. - 2004. - Vol. C69. - P. 034315.

НАБЛИЖЕННЯ СЕРЕДНЬОГО ПОЛЯ В СКІНЧЕНИХ ЯДРАХ ТА ЯДЕРНІЙ МАТЕРІЇ

Ш. Шломо

Обговорюється підгонка параметрів сил Скірма, виходячи з експериментальних даних для основного стану нормальних та екзотичних ядер. Зокрема, для підгонки використано значення радіусів орбіт валентних нейтронів та енергій продихових мод кількох ядер. На значення параметрів Скірма накладено додаткові обмеження, зумовлені вимогою позитивності нахилу енергії симетрії *S*, коефіцієнта підсилення κ, що пов'язаний з гігантським дипольним резонансом, та параметра Ландау $G_0^{'}$. Наведено результати розрахунку силової функції збудження продихової моди в рамках теорії Хартрі - Фока з використанням наближення випадкових фаз. Обговорюється стан досліджень модуля стиснення ядерної матерії.

ПРИБЛИЖЕНИЕ СРЕДНЕГО ПОЛЯ В КОНЕЧНЫХ ЯДРАХ И ЯДЕРНОЙ МАТЕРИИ

Ш. Шломо

Обсуждается подгонка параметров сил Скирма на основе экспериментальных данных для основного состояния нормальных и экзотических ядер. В частности, при подгонке использованы величины радиусов орбит валентных нейтронов и энергии дыхательных мод нескольких ядер. На величины параметров Скирма были наложены ограничения, обусловленные требованием положительных значений наклона энергии симметрии *S*, коэффициента усиления κ, связанного с гигантским дипольным резонансом, и параметра Ландау $G_0^{'}$. Представлены результаты расчета силовой функции возбуждения дыхательной моды в рамках теории Хартри - Фока с использованием приближения случайных фаз. Обсуждается состояние исследований модуля сжатия ядерной материи.

Received 09.06.08,
revised - 10.12.08.